An Active 3-Dimensional Localization Scheme for Femtocell Subscribers Using E-UTRAN

Mohammed Aquil Mirza, Muhammad Zeeshan Shakir, and Mohamed-Slim Alouini
Electrical Engineering Program, King Abdullah University of Science and Technology (KAUST)
Thuwal 23955-6900, Makkah Province, Kingdom of Saudi Arabia
Email: {aquil.mohammed, muhammad.shakir, slim.alouini}@kaust.edu.sa

***Abstract*—Femtocells provide an efficient solution to overcome the indoor coverage problems and also to deal with the traffic within Macro cells. The possibility of localizing femtocell subscriber stations based on the timing ranging advance parameter (TRAP), obtained from E-UTRAN (Evolved UMTS Terrestrial Radio Access Network), within the network signal internals is challenging and is studied throughout in this paper. The principle approach to localization based on Euclidean distances from multiple base stations is outlined. We investigate the specifications of the timing parameters or TRAP used for air interface of 4G network as they relate to calculating the subscriber distances. Computer simulation is used to demonstrate the localization accuracy using multiple base station networks when estimating likely locations of femtocell subscribers stations on a two-dimensional coordinate mapping system. However, we further extend our simulations to demonstrate expected location accuracy of subscriber stations, for multiple base station networks, on a three dimensional coordinate mapping scheme. The possibility of of error-fixes shows eight times greater accuracy than in previous results is expected to achieve by applying timing advance techniques to Global System for Mobile communications networks, by using a two-dimensional coordinate mapping scheme. We later compare our study with the effect of global positioning system (GPS) by using a three-dimensional coordinate mapping scheme, which is predicted to give an 72.4 cms accuracy of subscriber station location.**

***Index Terms*—Femtocell, Localization, LTE, 3GGP.**

I. Introduction

Wireless Communications demand for higher data rates and has led to the development of new cellular standards like WiMAX (802.16e), the Third Generation Partnership Project's (3GPP's) High Speed Packet Access (HSPA) and Long Term Evolution (LTE) [1], [2]. Femotocell is a small cellular base station (BS), especially designed for home and business areas [3]. Femtocells are low-power, low-cost and user deployed home base stations that can improve poor indoor coverage and enhance system capacity. In 3GGP technology, a Home NodeB (HNB) is a 3G femtocell, whereas, a Home eNodeB (HeNB) is an LTE femtocell. Typically the range of a microcell is less than 2 Km wide, a picocell is 200 m or less, and a femtocell is on the order of 10 m.

The two major limitations of wireless communication are range and capacity. Cellular service is far superior in areas of high population density compared to scarcely populated areas. The initial cellular systems were designed for a single application, voice, but today with the advent of fourth generation (4G) cellular systems, users expect good quality of voice, uninterrupted voice calls, clear video images, faster downloads and precise positioning system. However, the localization of the femtocells subscribers is still an open issue as 4G suffers from inadequate indoor signal penetration, leading to poor coverage in the indoor environment where users spend most of their time. These characteristics indicate that future cellular wireless systems must be designed in a different way, hence the motivation to move towards smaller cells that operate in a licensed spectrum but are privately owned. Femtocells provide a good solution to overcome indoor coverage problems and also to deal with the traffic within Macro cells [4]. The possibility of localizing a femtocells subscriber station based on TRAP [5] within the network signal internals is studied throughout this paper.

The basic approach to localization based on Euclidean distances from multiple base stations is studied in [6], which proves out to be very energy expensive. We investigate the specification of the timing parameters used for 4G network entry as they relate to calculating the subscriber distances. Computer simulation (using MATLAB) is used to demonstrate expected localization accuracy in multiple base station networks when estimating likely locations of subscriber stations on a three-dimensional coordinate mapping system.

II. Proposed Scheme

Femtocells beholds a TRAP or time ranging (TR) parameter similar to GSM and timing adjust (TA) as in WiMAX. The TRAP is the key solution for geolocalization for femtocell subscribers. If the timing of any subscriber needs modification then the network generates a TA command instructing the subscriber to increase or decrease its timing relative to current uplink timing. The user specific TA is transmitted as a (Medium Access Control) MAC control element on the downlink-shared channel (DLSC). In this paper, we imply the same principles of WiMAX for the knowledge of signal in relation to TA data to isolate the subscriber location based on the radial distances known to the BS locations.

The TA data is hidden in the transmitted signals and we use the computer simulation to validate and extract this data with multiple BS scenarios under variable conditions such as placing the subscriber at random distances and at random angles from the BS. Femtocells uses several multiple access schemes for uplink and downlink. They are signal carrier frequency division multiple access schemes (SCFDMA) and

978-1-4673-0990-5/12/$31.00 ©2012 IEEE

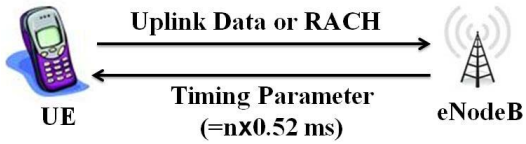

Fig. 1. Uplink timing control

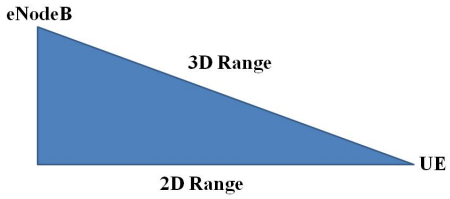

Fig. 2. 2D and 3D localization ranges

orthogonal frequency division multiple access (OFDMA) [7]. These schemes allows several subscriber station or user equipment (UE), to share the capacity of the network.

Femtocells uses the two modes of operation for uplink and downlink sharing the same frequency band for transmission and reception: frequency-division duplexing (FDD) and time-division duplexing (TDD). The major difference between the two schemes is the use of paired and unpaired frequency bands respectively. The eNodeB uses the TA control sequence so that the transmissions from the uplink mode arrives within cyclic prefix. The eNodeB continuously measures the timing using random access channel (RACH) of UE uplink signal and adjusts the uplink transmission as shown in Fig. 1.

A. Timing Advance Calculation for Femtocells

A standard 3GGP unit of time is used throughout our calculations and we express the sampling time as, $T_s = 1/(S_s \times FFT_{max})$ Seconds. Where S_s is the subcarrier frequency of 15 KHz and FFT_{max} is the maximum FFT size, which is 2048. We then divide the radio frame structures of uplink and downlink with duration of T_s and calculate the the radio frame, T_f as a product of T_s and 30.72 MHz sampling frequency such that $T_f = 307200 \times T_s = 10$ ms. Radio frames are subdivided into slots. These slots are expressed in time domain as $T_{slot} = 15360 \times T_s = 0.52$ ms.

3GGP-TS 36.213 standard gives further refinement on transmission timing adjustments, where TA command indicates the change of uplink timings, relative to current uplink timing, in the multiples of $16T_s$. MAC random access responses uses 11-bit TA command T_A indicates N_{TA} values by index values of $T_A = 0, 1, 2, ..., 1282$, then the timing alignment is given as $N_{TA} = 16T_A$. As for N_{TA} this corresponds to the number of TRAP or TA units that need to be applied to the start times of uplink and downlink radio frames and this gives a maximum of 20512 TA units. In some cases, 6-bit TA command indicates adjustment of the current N_{TA} value $N_{TRAP,old}$ to the new T_A value $N_{TA,new}$ where we define $N_{TA,new} = N_{TA,old} + 16(T_A - 31)$ where $T_A = 0, 1, 2, ..., 63$. It is observed here that adjustment of N_{TA} by a positive or negative amount indicates the increase or decrease of uplink transmission timing by a certain amount. With this calculation one can achieve the time and distance with respect to one unit of TA. Literature review predicts the value of TA as 0.67 ms [8] correlating to radial distance of 100 m from eNodeB to UE. For correctness of this value we used the formula as below;

$$N_{TA} + N_{TAoffset} \times T_s = (20512 + 0) \times 1/(15000 \times 2048) = 0.672ms \quad (1)$$

The distance for per unit of TA is derived using the sampling frequency of 3GGP. Different sampling frequencies are listed in [8]. Then we calculate the final distance as, Distance = (c/f_s), where c is the speed of light. Then each unit of TA should correlate to a distance of 78.14 m. The maximum index value (1282) when multiplied by 78.14 m produces a distance of 100.17 Km, thereby validating the assertion found in literature. In our simulation model we apply this calculated distances to normalize the intersecting radii.

B. Approach for Range Approximations

In this section, we try to derive the approximations needed for calculation of the 3D distance between eNodeB and UE as shown in Fig. 2. Since, eNobeBs and UE uses the TA-based radius which proves out to be more precise than 2D coordinate system. The illustration of the difference between 2D and 3D is shown as below. However, the z-axis varies between UE and eNodeB and hence it leaves an error. We try to employ the method of triangulation for determining the relative position of UE's from respective eNodeB. 3D approximations requires the trilateration of spheres rather than circles as in 2D case. This technique is used by GPS, where satellite in space acts as a center point for the spheres. The estimated point of intersection of three or more satellite spheres gives the likely location of the GPS device. For calculating the 3D ranging we need to determine the height(z-axis) from the center of the sphere of the eNodeB.

In range approximation we employ three parameters. Firstly, we employ a flat earth model whose calculation are based on Cartesian coordinates [9]. This provides a coordinate system with simplified calculations of range radii, intercept points and probability polygons. The flat model's typical error over the geode is very small even after a coordinate transformation. Secondly, intersecting radii is based on the propagation delay of the signals, as calculate in the section above. The range radii calculations uses a the best scenario with an absolute TA by amount of 78.14 with no variance and standard deviation The last parameter offsets the best case scenario by using deviation of range radii calculations. The study of 3GGP specifications leads us to the establishment of real-world value of deviation as 78.14 m.

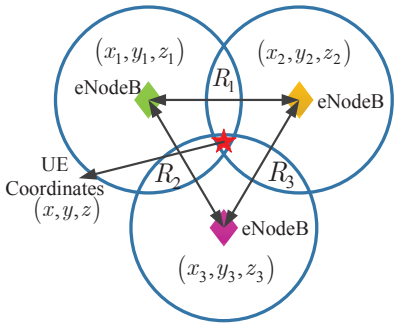

Fig. 3. Node locations in 3D sphere scenario

C. Node Location Calculations

With two eNodes having the known radius the likely location of an UE is the point of intersection of radius rings. Here we take into account the three possible scenarios (shown in figure below); two radius of spheres are separated without touching, one sphere completely inside another and radius sphere that intersect each other. When two spheres intersect then there is an additional plane with vast number of intersection points. Henceforth, we introduce a third sphere to calculate the point of intersection that localize the UE.

We developed a algorithm using triangulation and law of cosines and we found spheres from eNodeBs using the TA-based radii, $X-Y$ plane coordinated of eNodeB and height of the eNodeB as on z-axis. This leads to a system of equations we used using linear algebra to determine the most common point of intersection. The Cartesian coordinates of the i-spheres equate to a system of following equation

$$(x - x_i)^2 + (y - y_i)^2 + (z - z_i)^2 = R_i^2 \tag{2}$$

where (x_i, y_i, z_i) corresponds to the intersecting center points of the spheres with R_i as the corresponding radii, calculated from [8] by using law of cosines and i represents the number of femtocell base stations. Once we substitute the values of center points and radii (for $i = 4$) we further reduce the system by subtracting the equation of first sphere from the equations of remaining two spheres. we obtain the following set of equations

$$\begin{aligned} 2[(x_2 - x_1)x + (y_2 - y_1)y + (z_2 - z_1)z] &= d_1 \\ 2[(x_3 - x_1)x + (y_3 - y_1)y + (z_3 - z_1)z] &= d_2 \\ 2[(x_3 - x_2)x + (y_3 - y_2)y + (z_3 - z_2)z] &= d_3 \end{aligned} \tag{3}$$

where $d_1 = R_1^2 - R_2^2 - x_1^2 + x_2^2 - y_1^2 + y_2^2 - z_1^2 + z_2^2$; $d_1 = R_1^2 - R_2^2 - x_1^2 + x_2^2 - y_1^2 + y_2^2 - z_1^2 + z_2^2$ and $d_3 = R_2^2 - R_3^2 - x_2^2 + x_3^2 - y_2^2 + y_3^2 - z_2^2 + z_3^2$

To find the common point of these intersection sphere we define a linear transformation of the form $\mathbf{A}x = b$. This is portrayed as

$$2\begin{bmatrix} (x_2 - x_1) & (y_2 - y_1) & (z_2 - z_1) \\ (x_3 - x_1) & (y_3 - y_1) & (z_3 - z_1) \\ (x_3 - x_2) & (y_3 - y_2) & (z_3 - z_2) \end{bmatrix} \begin{bmatrix} x \\ y \\ z \end{bmatrix} = \begin{bmatrix} d_1 \\ d_2 \\ d_3 \end{bmatrix}$$

where matrix $\mathbf{A}$ holds the coefficients and b holds the constants from (3) and x are the unknown coordinates for the intersection (x, y, z).

The unknown point is calculated as $x = \mathbf{A}^{-1}b$. But the inverse of matrix is possible only for square matrix. When A is not a square matrix we find the solution by using the least squares or best-fit-in solution by using normal equation, $\mathbf{A}^T\mathbf{A}x = \mathbf{A}^T b$, which gives a unique solution $\hat{x} = (\mathbf{A}^T\mathbf{A})^{-1}\mathbf{A}^T b$ and $\hat{x}$ is the unique solution to least squares method. In the following section we use the following results to simulate our cased for multiple BS.

III. Simulation Results

In this section, we try to study our model for three BS, four BS and for multiple BS. In this first approach we use 3 eNodeB radii to approximate the location of a UE. In all cases the true position of the UE's is set at origin on the $X - Y$ axis. The simulation creates eNodeB at varying degrees each with normally distributed at random distance with a mean of 1 Km from UE and a standard deviation of 300 m and the TA is maintained at 78.14 m. TA being a discrete value the eNodeB rounds the radial distance to whole unit of TA. A monte carlo simulation of 1,00,000 iterations were conducted for each with an degree increment of 10 degrees ranging from 0 to 180 degrees.

We observe that most accurate approximation of the UE location occurs at 180 degrees when the placement of the eNodeB and the UE form a straight line with each other. Tower height of the eNodeB was generated with normally distributed random heights with a mean of 300 m from the ground plane with a standard deviation of 250 m to facilitate a minimum eNodeB height of 50 m. Trials from Monte Carlo were recorded and we then apply the quantization error. In this case the accuracy was tested and compared with the simulation results without errors. We observe that standard deviation to TA and quantization error to radii had little effect on the approximation error.

A mean radial spherical error (MRSE) analysis was also conducted and the results are shown in Fig. 4 and Fig. 5. MRSE is calculated by summing the variances of X, Y and Z coordinates of all 1,00,000 Monte Carlo simulations and the square root value is obtained. The radial value of MRSE centered on the origin and the actual UE location shows 61% of the location values are contained. An estimate error for multiple femtocell stations is studied in these graphs.

The next simulation investigates the case for 4 eNodeB network. The same parameters are used that were used for 3 eNodeB network. With the addition of the fourth node the location accuracy increases and is shown in Fig. 6.

The final simulation is done for multiple eNodeB, as shown in Fig. 7, and in turn test the approximation accuracy. Firstly,

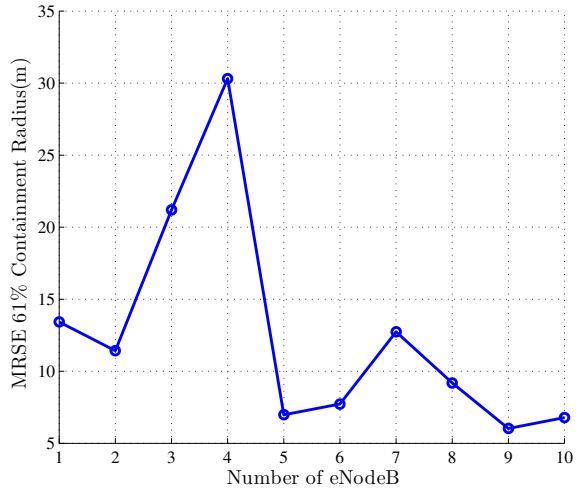

Fig. 4. MRSE with three eNodeB

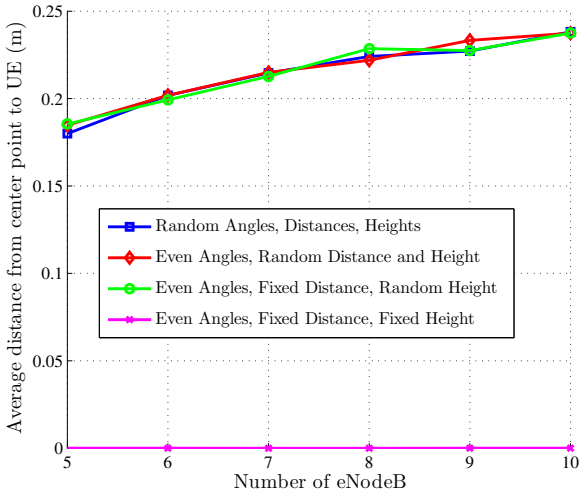

Fig. 5. MRSE with multiple eNodeB

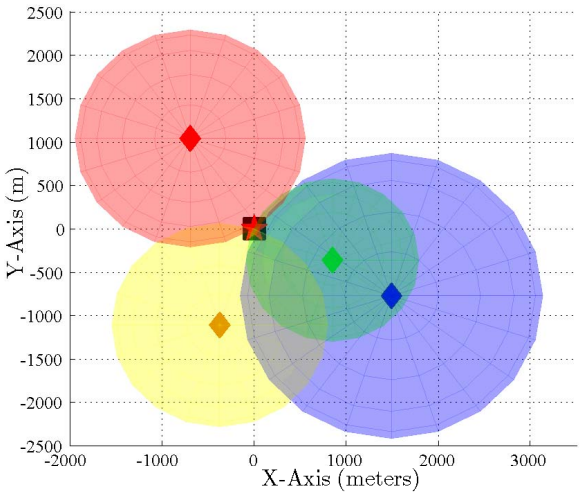

Fig. 6. 4 Femtocells with an UE. (where *rhombus* represent the femtocell BS and *square* is femtocell subscriber station location and *star* represents the actual calculated position of eNodeB)

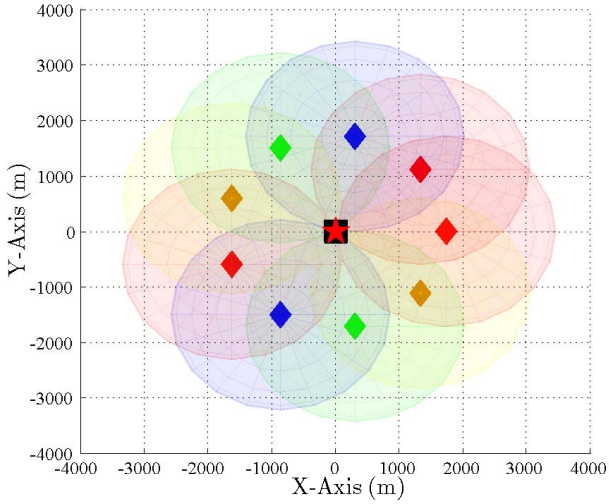

Fig. 7. Example of accurate location estimate with 9eNodeB network

eNodeB were placed in random angles in relation to the UE at the origin. Distances of eNodeB is 1.2 Km with a standard deviation of 400 m. Tower heights are generated with a mean of 300 m and with a standard deviation of 250 m, which facilitate the height of 50 m. The largest approximation error occurs with 4 eNodeB network but the margin of approximation error with five or more nodes remained consistent despite of the additional tower heights. This leads to an interesting fact that a system of equations is precise in case of 2 eNodeB.

REFERENCES

[1] J. S. E. Dahlman, S. Parkvall and P. Beming, *3G Evolution: HSPA and LTE for Mobile Broadband*, 2nd ed. Burlington, Massachusetts: Elsevier Ltd., 2008.

[2] "Front matter," pp. i–xxxv, 2009. [Online]. Available: http://dx.doi.org/10.1002/9780470742891.fmatter

[3] V. Chandrasekhar, J. Andrews, and A. Gatherer, "Femtocell networks: a survey," *Communications Magazine, IEEE*, vol. 46, no. 9, pp. 59 –67, september 2008.

[4] Y. Shi, A. MacKenzie, L. DaSilva, K. Ghaboosi, and M. Latva-aho, "On resource reuse for cellular networks with femto- and macrocell coexistence," in *Global Telecommunications Conference (GLOBECOM 2010), 2010 IEEE*, dec. 2010, pp. 1 –6.

[5] M. Spirito and A. Mattioli, "Preliminary experimental results of a gsm mobile phones positioning system based on timing advance," in *Vehicular Technology Conference, 1999. VTC 1999 - Fall. IEEE VTS 50th*, vol. 4, 1999, pp. 2072 –2076 vol.4.

[6] H. Breu, J. Gil, D. Kirkpatrick, and M. Werman, "Linear time euclidean distance transform algorithms," *Pattern Analysis and Machine Intelligence, IEEE Transactions on*, vol. 17, no. 5, pp. 529 –533, may 1995.

[7] G. Berardinelli, L. Ruiz de Temino, S. Frattasi, M. Rahman, and P. Mogensen, "Ofdma vs. sc-fdma: performance comparison in local area imt-a scenarios," *Wireless Communications, IEEE*, vol. 15, no. 5, pp. 64 –72, october 2008.

[8] "Lte-dl-src (downlink baseband signal source)," 2010.

[9] T. Steinar and Schei, "A finite-difference method for linearization in nonlinear estimation algorithms," *Automatica*, vol. 33, no. 11, pp. 2053 – 2058, 1997.